Simultaneous Three-Band Modulation and Fiber-Optic Transmission of 2.5-Gb/s Baseband, Microwave-, and 60-GHz-Band Signals on a Single Wavelength

Kensuke Ikeda, *Student Member, IEEE*, Toshiaki Kuri, *Member, IEEE*, and Ken-ichi Kitayama, *Fellow, IEEE, Member, OSA*

***Abstract*—Simultaneous modulation of 2.5-Gb/s baseband, microwave-band, and 59.6-GHz 155.52-Mb/s differential phase-shift keying signals on a single wavelength, using a single 60-GHz-band electroabsorption modulator (EAM), and fiber-optic transmission over a 40-km-long dispersion-shifted fiber (DSF) was experimentally demonstrated. The optimum operating conditions for three-band modulation and transmission were theoretically investigated. Degradation due to the nonlinearity of the EAM for the millimeter-wave signal is discussed theoretically. The fading problem due to the fiber dispersion of the standard single-mode fiber and the DSF was also investigated.**

***Index Terms*—Digital/analog signals hybrid transmission, electroabsorption modulator (EAM), millimeter-wave radio, optical access network, radio-on-fiber (ROF).**

I. Introduction

THE demand for broadband services in both fixed and mobile access networks is accelerating. Along with demand for various types of fixed wired access, such as fiber-to-the-home (FTTH) and xDSL, as well as fixed wireless access (FWA), there is also likely to be growing demand for either portable or mobile access to *wireless last hop* for mobile computing, personal digital assistants, and cellular phones. Microwave of the 2.4- and 5.2-GHz bands (IEEE 802.11 b, g, and a) is used commercially for wireless local-area networks (LANs). Millimeter-wave is also likely to be a strong candidate for providing radio-frequency (RF) resources, not only for fixed access systems such as dedicated short-range communication (DSRC) and FWA but also for portable or mobile access. Exploitation of millimeter-wave could provide broadband services and resolve the problem of frequency resources. The potential of radio-on-fiber (ROF) systems, which apply subcarrier-multiplexing (SCM) techniques to realize cost-effective millimeter-wave wireless access networks, has been investigated. One of the challenges is to enable FTTH and ROF systems to share a single optical fiber network. Simultaneous modulation and transmission of an FTTH baseband signal and a millimeter-wave SCM signal of ROF has been studied [1]–[5].

Manuscript received April 14, 2003; revised September 16, 2003. This work was supported by "Support System for R&D Activities in Info-Communications Area" under the Telecommunications Advancement Organization of Japan.

K. Ikeda and K. Kitayama are with the Department of Electronics and Information Systems, Graduate School of Engineering, Osaka University, 565-0871 Osaka Japan (e-mail: ikeda@eie.eng.osaka-u.ac.jp; kitayama@comm.eng.osaka-u.ac.jp).

T. Kuri is with the Basic and Advanced Research Division, Communication Research Laboratory, 184-8795 Tokyo, Japan (e-mail: kuri@crl.go.jp).

Digital Object Identifier 10.1109/JLT.2003.821739

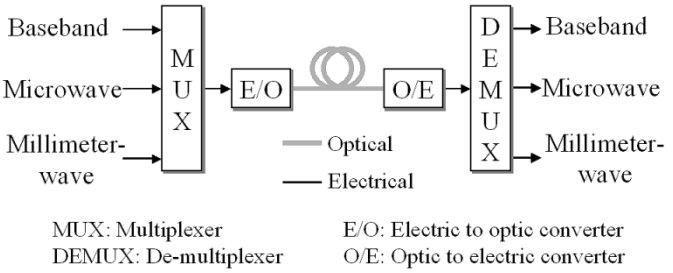

Fig. 1. Schematic block diagram for three-band modulation and transmission.

In this paper, we theoretically analyze and experimentally demonstrate simultaneous multiband modulation and fiber-optic transmission of a 2.5-Gb/s baseband signal, the sinusoidal wave of a microwave signal, and a 59.6-GHz 155.52-Mb/s differential phase-shift keying (DPSK) signal. An electroabsorption modulator (EAM) is the key to electrical-to-optical (E/O) conversion over a wide range from dc to the 60-GHz band [6]. Simultaneous modulation of 10-Gb/s baseband and 60-GHz-band signals has been demonstrated [1]. To the authors' knowledge, this is the first experimental demonstration of simultaneous modulation of multiband signals of 2.5-Gb/s baseband, microwave-band, and 60-GHz-band signals using a single EAM, with the optical signal transmitted on a single wavelength over a 40-km-long dispersion-shifted fiber (DSF). The influences between baseband and millimeter-wave signals have been reported previously [1]. Therefore, in this paper, we focus on the influence of a microwave signal on baseband and 60-GHz-band signals. This technique has potential for future FTTH access networks combined with wireless access supported by an ROF wireless feeder.

II. Three-Band Modulation and Transmission Scheme

Fig. 1 shows a conceptual configuration of the three-band modulation and transmission. A combined electrical signal comprising a baseband signal $b(t)$ [$= 1$ or -1], a microwave-band signal $\cos(2\pi f_{\mathrm{MIC}}t + \theta_{\mathrm{MIC}}(t))$, and a millimeter-wave-band RF signal $\cos(2\pi f_{\mathrm{MM}}t + \theta_{\mathrm{MM}}(t))$ is

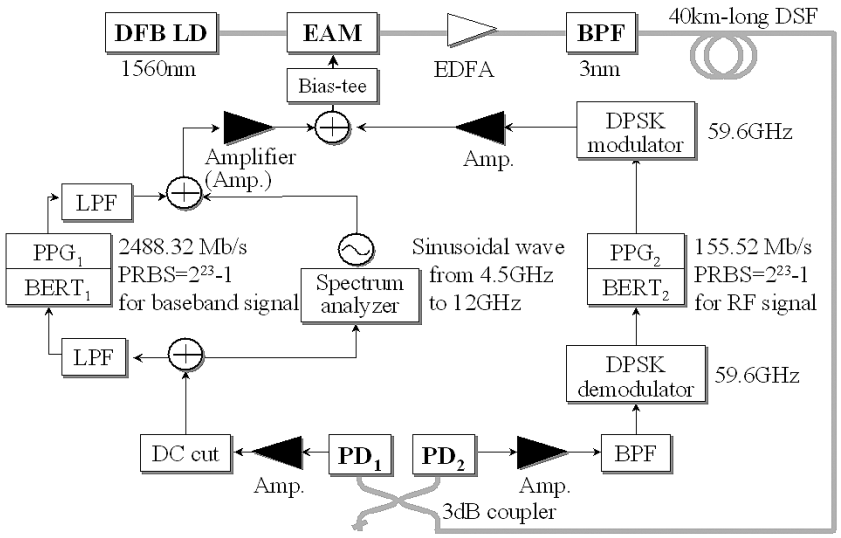

Fig. 2. Experimental setup for three-band modulation and transmission.

applied to the E/O converter as a modulation signal. f_{MIC} and f_{MM} are the carrier frequencies of the microwave- and millimeter-wave-band signals, respectively. $\theta_{\mathrm{MIC}}(t)$ [$= 0$ or π] and $\theta_{\mathrm{MM}}(t)$[$= 0$ or π] are the data for the microwave- and millimeter-wave-band signals, respectively. Here, it is assumed that the data rate of $\theta_{\mathrm{MIC}}(t)$ and $\theta_{\mathrm{MM}}(t)$ is slower than that of $b(t)$. The combined electrical signal is expressed by

$$M(t) = A\cdot\cos(2\pi f_{\mathrm{MM}}t+\theta_{\mathrm{MM}}(t)) + B\cos(2\pi f_{\mathrm{MIC}}t+\theta_{\mathrm{MIC}}(t)) + C\cdot b(t). \quad (2.1)$$

Here A, B, and C are the amplitudes of the millimeter-wave-band, microwave-band, and baseband signals, respectively. It is assumed that the millimeter-wave-band, microwave-band, and baseband signals are separable. A single-mode light source emits an optical carrier with a power of P, frequency of f_c, and phase noise of $\phi_{pn}(t)$. If transmitting over a optical fiber on the z-axis, the complex amplitude of the optical carrier $e_c(t,z)$ is generally expressed by [7]

$$e_c(t,z) = \sqrt{2P}\cdot\exp\{j\phi_c(t.z)\} \quad (2.2)$$

$$\phi_c(t,z) = \omega_c t-\beta(\omega_c)z \quad (2.3)$$

$$\omega_c \equiv \frac{\partial\phi_c(t,z)}{\partial t} = 2\pi f_c+\frac{d\phi_{pn}(t)}{dt} \quad (2.4)$$

where $\beta(\omega)$ is the propagation constant as a function of the angular frequency and is approximately expanded as

$$\beta(\omega_c\pm\Delta\omega)\approx\beta_0\pm\beta_1\cdot\Delta\omega\pm\frac{1}{2}\beta_2\cdot(\Delta\omega)^2\pm\frac{1}{6}\beta_3\cdot(\Delta\omega)^3 \quad (2.5)$$

where $n(\omega)$ and c are the refraction index and the velocity of light in the vacuum. In this expression, β_0 and β_1 are the inverse of the phase and group velocities, respectively. Then, β_2 is related to the dispersion D as follows [8]:

$$\beta_2 = -\frac{\lambda^2}{2\pi c}\cdot D. \quad (2.6)$$

Although β_m for $m\geq 3$ generally relates to higher order dispersion, higher order dispersion is neglected because it does not seriously affect the system performance of access networks in which ultrashort pulses are not treated. The optical carrier $e_c(t,0)$ is intensity-modulated with an E/O converter using a combined electrical signal $M(t)$. To avoid overmodulation, $|M(t)|$ should be less than one. In this condition, A, B, and C correspond to the modulation indexes for the millimeter-wave-band, microwave-band, and baseband signals, respectively. They should then satisfy $A+B+C\leq 1$. The modulated signal after the transmission of $z=L$ is given by

$$e(t,L) = \left[\frac{1}{2}(1+M(t))\right]^{\gamma}\cdot e_c(t,L). \quad (2.7)$$

where γ is the complex value defined by the chirp parameter of the optical modulator α as follows [9]:

$$\gamma = \frac{1+j\alpha}{2} \quad (2.8)$$

$$I(t,L) = \frac{eR}{hf_c}\overline{|e(t,L)|^2}\propto\frac{R}{2}\overline{|e(t,L)|^2} \quad (2.9)$$

where $-e$, R, and h are an electron charge, the photosensitivity of the optical-to-electrical (O/E) converter, and the Planck constant, respectively. Here, the definition of power $\overline{|e_c(t,L)|^2} = \overline{|e_c(t,0)|^2}$ is used under no fiber dispersion

$$I(t,L)|_{\text{at around Millimeter wave}} \propto RPA\cdot\sqrt{1+\alpha^2}\cdot\sqrt{1+\frac{1+\alpha^2}{4}\cdot C^2+C\cdot b(t)} \cdot\cos\phi_{\mathrm{dMM}}(t)\cdot\cos\left(2\pi f_{\mathrm{MM}}(t-\beta_1 L)+\theta_{\mathrm{MM}}(t-\beta_1 L)\right), \quad (2.10)$$

$$I(t,L)|_{\text{at around Microwave}} \propto RPB\cdot\sqrt{1+\alpha^2}\cdot\sqrt{1+\frac{1+\alpha^2}{4}\cdot C^2+C\cdot b(t)} \cdot\cos\phi_{\mathrm{dMIC}}(t)\cdot\cos\left(2\pi f_{\mathrm{MIC}}(t-\beta_1 L)+\theta_{\mathrm{MIC}}(t-\beta_1 L)\right), \quad (2.11)$$

$$I(t,L)|_{\text{at around Baseband}} \propto RP\left[1+\frac{1+\alpha^2}{2}\cdot C^2+Cb(t)\right]\overset{DC\text{-}cut}{\approx}RPC\cdot b(t) \quad (2.12)$$

where

$$\begin{aligned}&\phi_{dMMorMIC}(t)\\&=\frac{\pi\lambda^2 DLf_{MMorMIC}^2}{c}+\arctan\frac{2\alpha}{2+(1+\alpha^2)C\cdot b(t)}\\&=\frac{\pi\lambda^2 DLf_{MMorMIC}^2}{c}+\arctan\alpha-\arctan\frac{\alpha\cdot C\cdot b(t)}{2+C\cdot b(t)}.\end{aligned}\tag{2.13}$$

These terms induce fading problems along the length of the fiber when the frequency of the transmitted RF signal is high and the dispersion parameter is not negligible. This phenomenon is treated in Section V-B. It is confirmed mathematically in (2.10)–(2.12) that baseband, microwave-band, and millimeter-wave-band signals are generated after O/E conversion. We used $b^2(t)=1$ in the above calculation.

III. Experimental Setup

Fig. 2 shows the experimental setup. In the transmitter, a baseband signal (2488.32 Mb/s, PRBS$=2^{23}-1$) was generated from a pulse pattern generator (PPG_1) and filtered by a quasi-Gaussian low-pass filter (LPF) with a cutoff frequency of 2.5 GHz. The bit-error-rate (BER) measurements for the microwave regime were not available. Instead, the influence of the microwave signal on the baseband and 59.6-GHz-band signals was investigated using a sweeping sinusoidal microwave signal ranging from 3.5 to 12.0 GHz. The sinusoidal wave of the microwave was generated by a synthesized RF oscillator. A 59.6-GHz RF signal (155.52 Mb/s, PRBS$=2^{23}-1$) was generated by another PPG_2 and a DPSK modulator. The sum of the baseband signal and the sinusoidal wave in the microwave was amplified and combined with the 59.6-GHz RF signal. The optical carrier ($\lambda=1560$ nm, 5.0 dBm) was modulated with a special class of 60-GHz-band EAM [6] by applying the combined signal. The bias of the EAM was set to -1.30 V, and the input V_{PP} of the baseband and 59.6-GHz band to the EAM was set to 0.49 and 0.46 V, respectively. The input V_{PP} of the microwave to the EAM varied from 0.11 to 0.67 V. The modulated optical signal was amplified using an erbium-doped fiber amplifier (EDFA). The excess amplified spontaneous emission (ASE) noise from the EDFA was suppressed by an optical bandpass filter (BPF). A 40-km-long DSF ($\lambda_0=1560.395$ nm) was used as a fiber-optic link for the purpose of reducing fiber dispersion effect during signal transmission. The received optical signals were detected by a photodetector (PD) and then demodulated for the 59.6-GHz band through a bandpass filter (BPF) to remove undesired frequency components. To regenerate the baseband data, the LPF suppressed the higher frequency components. A cunning-clock was used to measure the BER of the baseband signal. A 3-dB optical coupler and two PDs were used instead of a single PD, and an electrical power divider was used to measure the BER of the baseband and 59.6-GHz band simultaneously.

Fig. 3(a) shows a comparison of the return loss of the EAM module for the RF input before and after trimming the stub in the 60-GHz-band [6]. This EAM was tailored to produce a peak response in the millimeter-wave region. The 15-dB reflection loss bandwidth of about 3 GHz (58.5–61.5 GHz) was wide enough

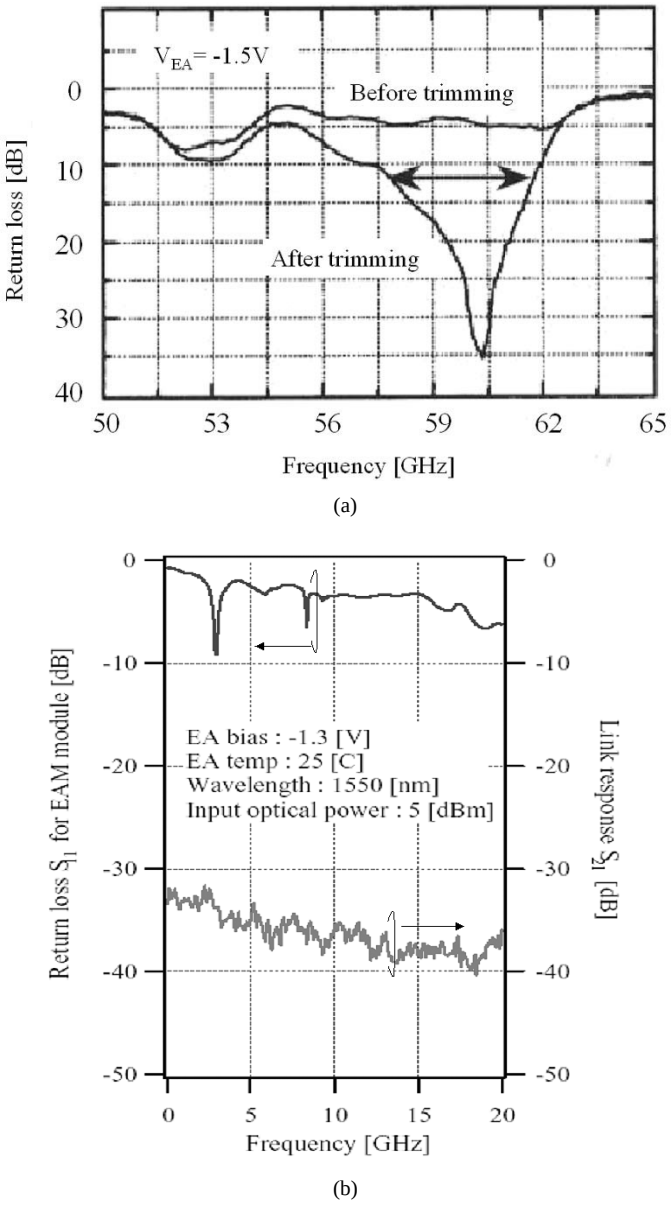

Fig. 3. Return loss of EAM module for RF input: (a) 50–65 GHz and (b) dc–20 GHz.

to put into the 155.52-Mb/s millimeter-wave signal. Fig. 3(b) shows the return loss and link response of the EAM module in a frequency of less than 20 GHz, which has been described elsewhere [1]. It is considered to indicate a similar response tendency, even in the case of 1560 nm. For our purposes, the frequency response has to be broadband from dc. The return loss of the EAM module in dc to 20 GHz is not so low, and this characteristic needs to be improved for the purpose of using an EAM as a broadband E/O. However, the link response does not have dip points. This shows the possibility of modulating baseband and microwave-band signals by feeding these signals to the EAM. The measured extinction ratio of the EAM is plotted in Fig. 4. The measured wavelength of the optical carrier was $\lambda=1560$ nm. The insertion loss was about 7 dB when the bias voltage of the EAM was set to -1.30 V.

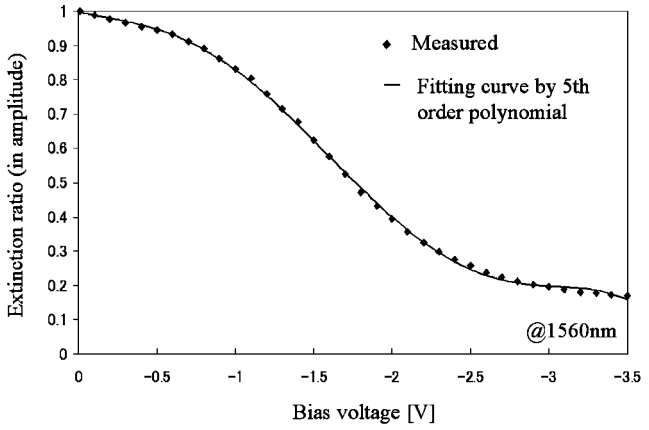

Fig. 4. Measured extinction ratio of EAM.

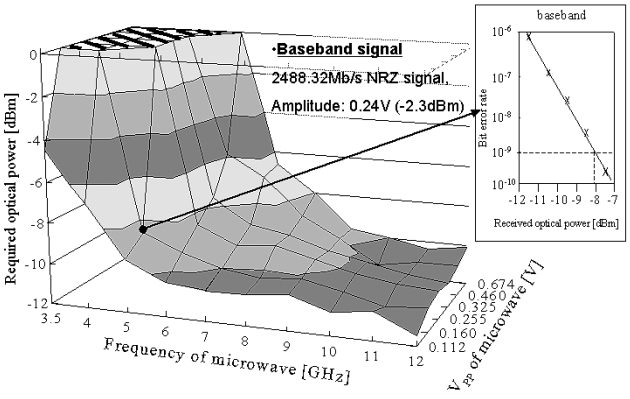

Fig. 5. Required optical power for baseband signal to achieve BERs below 10^{-9}.

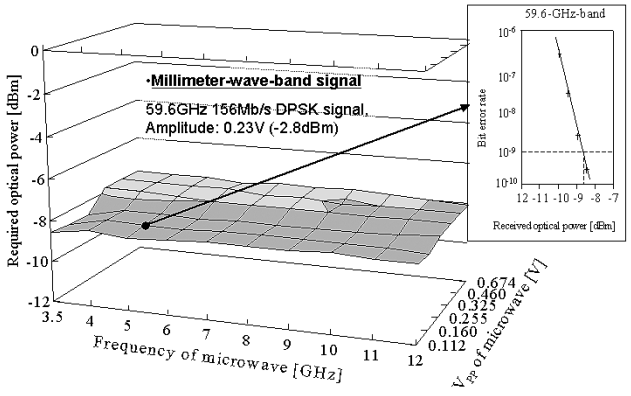

Fig. 6. Required optical power for 59.6-GHz-band signal to achieve BERs below 10^{-9}.

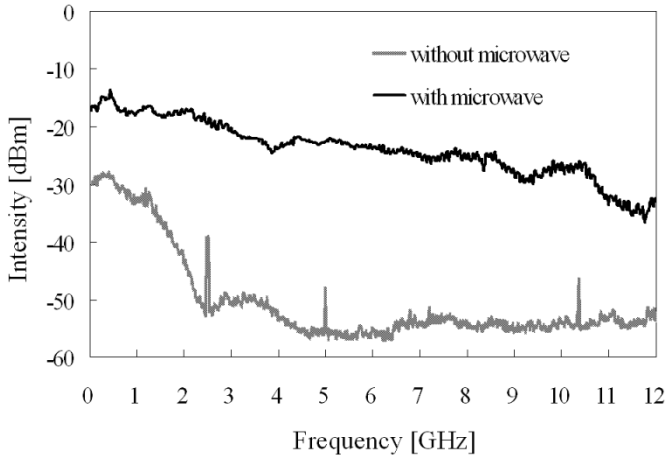

Fig. 7. Intensities of swept microwave versus frequency.

IV. Experimental Results

We investigated the operating conditions required for successful three-band transmission. Fig. 5 shows the required optical power for the 2.5-Gb/s baseband signal to achieve BER$=10^{-9}$ as a function of the frequency and applied voltage of the microwave signal. The BER of the baseband signal when the microwave V_{pp} and frequency were 0.160 V and 5 GHz, respectively, is shown as an example. Note that BER$< 10^{-9}$ for the baseband signal was maintained except in the region of a low V_{pp} of around 4 GHz (oblique lines). The frequency of the microwave signal was set to 3.5–12.0 GHz and the applied voltage (V_{PP}) was set to 0.11-0.67 V; they were measured on input to the EAM. We can see a tendency for the required power to decrease with a higher frequency and smaller amplitude. Fig. 6 shows the required optical power for the 59.6-GHz signal as a function of the frequency and applied voltage of the microwave signal. The BER for the baseband signal when the microwave V_{pp} and frequency were 0.160 V and 5 GHz, respectively, is shown as an example. Here, BER$< 10^{-9}$ for the 59.6-GHz signal was maintained over the entire microwave frequency region when the received optical power was more than -7.8 dBm. Fig. 7 shows the microwave power at the output of the PD as a function of the frequency. The frequency was swept from 10 to 12 GHz, and its V_{PP} was fixed at 0.16 V, corresponding to a power of 0 dBm. The baseband signal achieved BER$< 10^{-9}$ when the frequency of the microwave was higher than 5 GHz and the V_{PP} of the baseband was set to 0.49 V. When the V_{PP} of the 59.6-GHz signal was set to 0.46 V, the 59.6-GHz signal always achieved BER$< 10^{-9}$. The microwave signal did not have a significant effect on the baseband signal when the microwave frequency was higher than 5 GHz. This is because in the frequency region above 5 GHz, the microwave was sufficiently suppressed by the electrical LPF in the baseband receiver. Since the microwave was also suppressed at the BPF before demodulation of the 59.6-GHz signal, it did not significantly affect the 59.6-GHz signal. Therefore, error-free (BER$< 10^{-9}$) simultaneous transmission of baseband and 59.6-GHz signals can be achieved if the power level of the microwave frequency is optimized. The link efficiency, which is defined as the power ratio of the output and input signals, was about -19 and -21 dB for the baseband and 5-GHz band, respectively. The insertion loss due to the optical link can be easily compensated by using commercial electrical amplifiers. This shows the feasibility of using our EAM for modulation and transmission of a microwave signal combined with baseband and 59.6-GHz signals.

Fig. 8(a) shows the BER of the baseband signal as a function of the received optical power for the back-to-back and 40-km-long DSF transmission with three-band modulation. These results show that there is no power penalty between back-to-back and 40-km-long transmission. In this case, we can see that fiber dispersion did not seriously affect the system

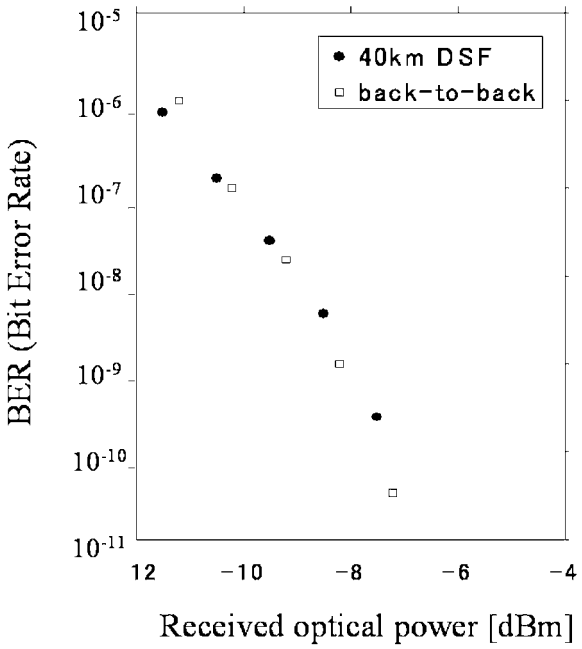

(a)

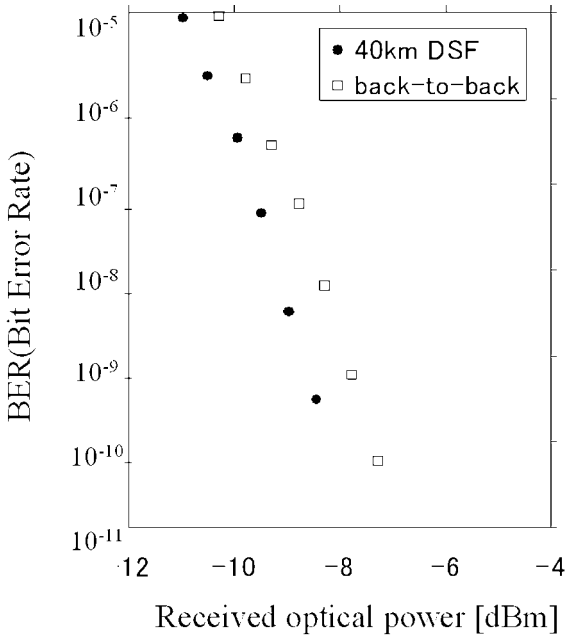

(b)

Fig. 8. (a) BERs of baseband signal and (b) BERs of 59.6-GHz-band signal.

performance of the baseband signal. It should be noted that fiber transmission of a baseband signal is free from fading problem due to chromatic dispersion, unlike fiber-optic transmission of a RF signal. Fig. 8(b) shows the BER for the 59.6-GHz signal in the back-to-back and 40-km-long DSF transmission with three-band modulation. A power penalty of about 0.7 dB was observed between the BERs for the 59.6-GHz-band signals in back-to-back and 40-km-long transmission because the positive dispersion of the DSF and the chirp parameter of the EAM improved the characteristics for these signals. When the

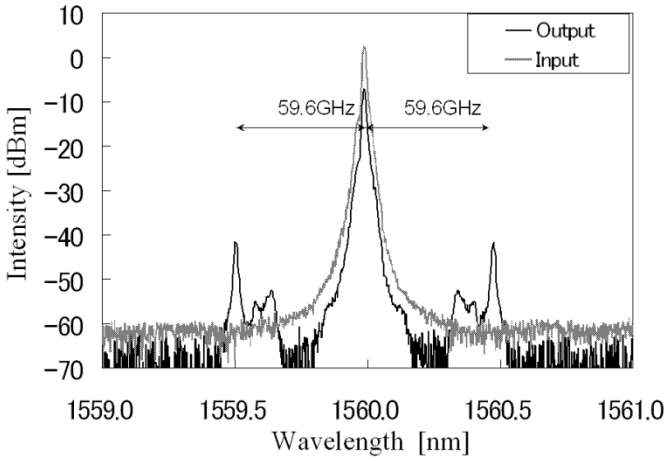

Fig. 9. Optical spectrum before and after EAM.

input electrical signals to the EAM were baseband signals of 0.49 V_{PP}, 59.6-GHz-band signals of 0.46 V_{PP} and 5.2 GHz, and a 0.16 V_{PP} sinusoidal wave, BER$< 10^{-9}$, was achieved.

Fig. 9 shows the optical spectra at the input and output of the EAM. An optical carrier with a wavelength of 1560 nm and a power of 5.0 dBm was generated by a tunable light source and put into the EAM. In this modulation, an optical double sideband signal is generated. The difference between the carrier intensity and subcarrier intensity was 34 dB, corresponding to the total modulation index of 7.8%. Undesired frequency components were observed inside the 59.6-GHz DSB signal. It is believed that these came from a millimeter-wave-band electrical amplifier.

V. Discussion

A. Signal Degradatiion due to EAM Nonlinearity

Here, we discuss the tendency for degradation of the millimeter-wave-band, microwave-band, and baseband signals due to the nonlinearity of the EAM. To simplify the theoretical analysis, the chirp parameter of the EAM, the laser phase noise, and fiber dispersion are neglected. We use a polynomial expression model for the extinction ratio of the EAM in the amplitude as previously described [1]

$$T(V(t)) = \sum_{n=0}^{\infty} a_n(V_b)(V(t) - V_b)^n \tag{5.1}$$

$$a_n(V_b) = \frac{T^{(n)}(V_b)}{n!}. \tag{5.2}$$

The input signal $V(t)$ is written as

$$V(t) = V_b + V_{BB} \cdot b(t) + V_{\mathrm{MIC}} \cos \phi_{\mathrm{MIC}}(t) + V_{\mathrm{MM}} \cos \phi_{\mathrm{MM}}(t) \tag{5.3}$$

where V_b, V_{BB}, V_{MIC}, V_{MM}, ϕ_{MIC}, ϕ_{MM}, and $b(t)$ are the bias voltage of the EAM, the amplitudes of the baseband, the microwave signals, the millimeter-wave signals, the phases of the microwave and the millimeter-wave signals, and the baseband data ($b(t) = 1$ or -1), respectively. V_{MM}, V_{MIC}, and V_{BB} have a relationship with A, B, and C in (2.1) as $A = V_{\mathrm{MM}}/V_b$,

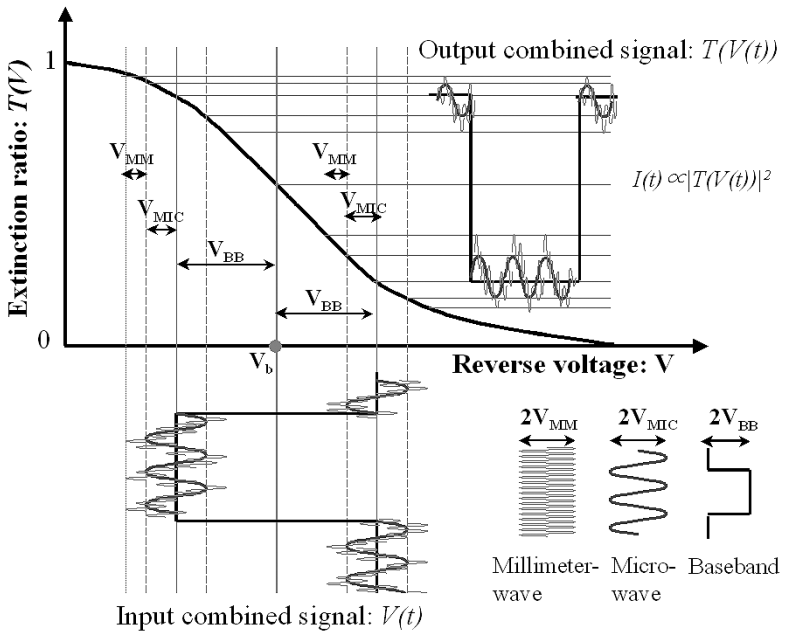

Fig. 10. Nonlinear extinction ratio and distortion of signal.

$B = V_{\mathrm{MIC}}/V_b$, and $C = V_{BB}/V_b$. The $T(V)$ satisfies $0 \leq T(V) \leq 1$. The modulated optical carrier is written as

$$e_c(t,z) = \sqrt{P} \cdot T(V) \cdot \exp\{j\phi_c(t.z)\} \tag{5.4}$$

where ϕ is the phase of the optical carrier. The photocurrents around baseband ϕ_{MIC} and ϕ_{MM} are estimated using the following equation:

$$I(t,z) \propto \overline{|c_c(t,z)|^2} \approx I_{DC}(t) + I_{\mathrm{MIC}}(t) + I_{\mathrm{MM}}(t). \tag{5.5}$$

Here, we introduce their evaluated signal powers expressed as

$$S_{BB} = R_L \overline{\left| |I_{DC}(t)|_{b(t)=1} - |I_{DC}(t)|_{b(t)=-1} \right|^2}, \tag{5.6}$$

$$S_{\mathrm{MIC}} = \frac{R_L\left(\overline{|I^2_{\mathrm{MIC}}(t)|_{b(t)=-1}} + \overline{|I^2_{\mathrm{MIC}}(t)|_{b(t)=1}}\right)}{2}, \tag{5.7}$$

$$S_{\mathrm{MM}} = \frac{R_L\left(\overline{|I^2_{\mathrm{MM}}(t)|_{b(t)=-1}} + \overline{|I^2_{\mathrm{MM}}(t)|_{b(t)=1}}\right)}{2} \tag{5.8}$$

where R_L is the load resistance and the probable equalities "-1" and "1" are assumed. To estimate degradation, we introduce the ratio

$$\Delta S_{BB} = \frac{S_{BB}}{|S_{BB}|_{V_{\mathrm{MIC}}=V_{\mathrm{MM}}=0}}, \tag{5.9}$$

$$\Delta S_{\mathrm{MIC}} = \frac{S_{\mathrm{MIC}}}{|S_{\mathrm{MIC}}|_{V_{BB}=V_{\mathrm{MM}}=0}}, \tag{5.10}$$

$$\Delta S_{\mathrm{MM}} = \frac{S_{\mathrm{MM}}}{|S_{\mathrm{MM}}|_{V_{BB}=V_{\mathrm{MIC}}=0}}. \tag{5.11}$$

The extinction ratio in the amplitude versus bias voltage and the distortion of the signals are illustrated in Fig. 10. V_b was set to -1.30 V, which is the same value as in the experiment. The extinction ratio $T(V)$ is expanded as

$$T(V) = a_0 + a_1(V - V_b)^1 + a_2(V - V_b)^2 + a_3(V - V_b)^3 + a_4(V - V_b)^4 + a_5(V - V_b)^5.$$

The measured extinction ratio of the EAM was used to decide a_n of (5.1) to calculate ΔS_{BB}, ΔS_{MIC}, and ΔS_{MM} numerically. $a_0 = 0.7129$, $a_1 = 0.4302$, $a_2 = -0.1114$, $a_3 = -0.1122$, $a_4 = 0.0317$, and $a_5 = 0.0194$ were used in (5.1). The approximation line shows good characteristics compared with the measured results shown in Fig. 4. The results for signal power degradation are shown in Fig. 11(a)–(c), respectively. In this analysis, it is assumed for simplicity that the link response is completely flat and the three frequency components are separable. The signals affect each other and degradations appear as the amplitude of the other signals increases. As the V_{PP} of the microwave becomes larger, the received optical power required for both the baseband and millimeter-wave signals to achieve BER$< 10^{-9}$ increases. However, the baseband signal is more robust than the microwave and millimeter-wave signals against the nonlinearity of the EAM. The millimeter-wave and microwave frequencies do not matter for this analysis because they are far away from each other. These numerical results predict well the tendencies shown in the experimental results.

B. Chirp Parameter and Fiber Dispersion Effects

Here, we investigate the relationship between the usable fiber length, the chirp parameter, and the fiber dispersion of SMF and DSF. The fiber length is assumed to be less than a few kilometers because it is generally known that there is a fading problem due to fiber dispersion in millimeter-wave ROF systems [6]. The fiber length at which RF signals cannot be detected appears periodically along the length of the fiber. In simultaneous three-band

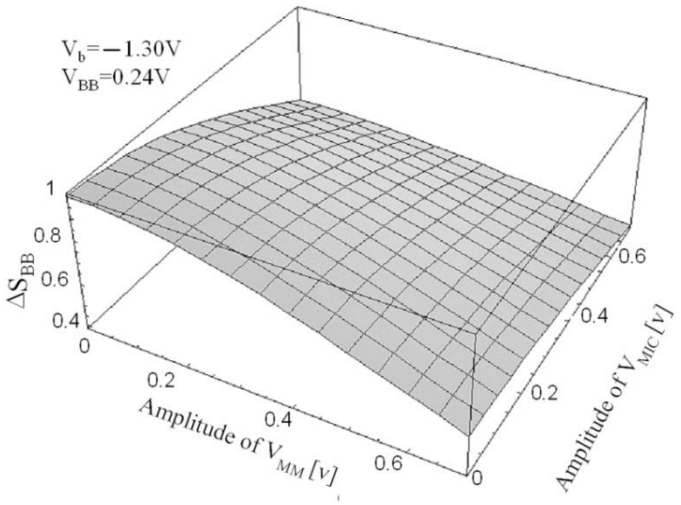

(a)

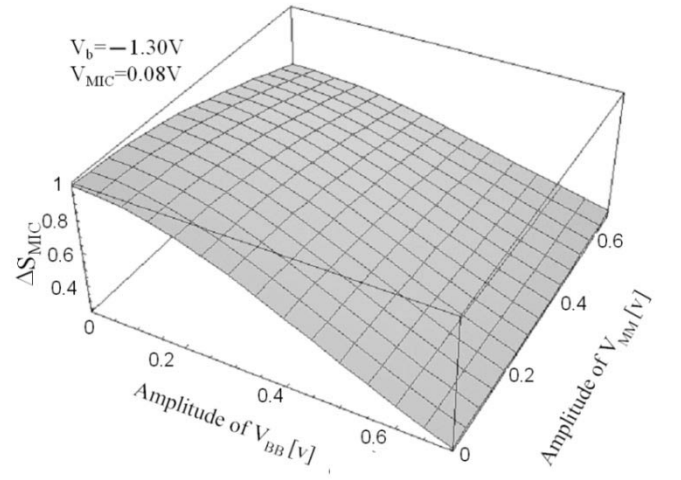

(b)

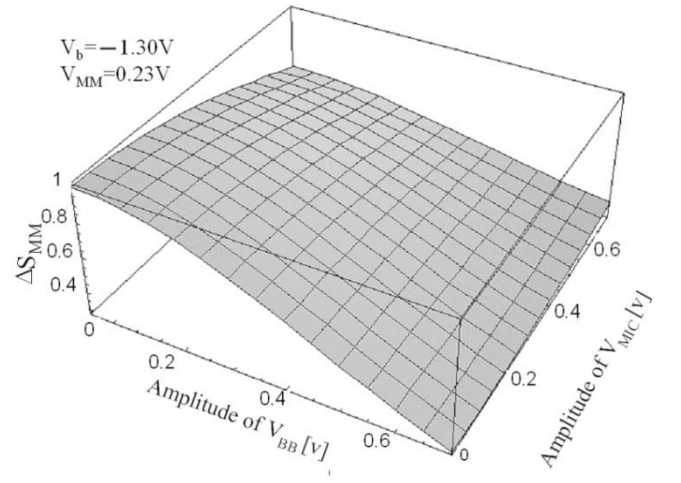

(c)

Fig. 11. Degradations for (a) baseband, (b) microwave, and (c) millimeter-wave signals.

modulation, the fading problem persists for microwave and millimeter-wave signals. As discussed previously, RF signal power

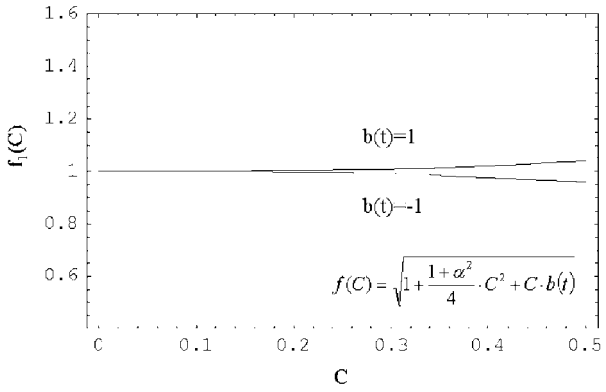

Fig. 12. Variation of $\sqrt{1+(1+\alpha^2)C^2/4+C\cdot b(t)}$ as a function of C.

fluctuates due to baseband signals. These problems are in (2.10), (2.11), and (2.13). The terms of RPA

$$\cdot\sqrt{1+\alpha^2}\cdot\sqrt{1+((1+\alpha^2)/4)\cdot C^2+C\cdot b(t)}\cdot\cos\phi_{\mathrm{dMM}}(t)$$

and RPB

$$\cdot\sqrt{1+\alpha^2}\cdot\sqrt{1+((1+\alpha^2)/4)\cdot C^2+C\cdot b(t)}\cdot\cos\phi_{\mathrm{dMIC}}(t)$$

are the amplitudes of the millimeter-wave-band and microwave-band signals, respectively. The parameters of R, P, A, B, C, and α are constant. Fig. 12 shows variation in the $\sqrt{1+((1+\alpha^2)/4)\cdot C^2+C\cdot b(t)}$ as a function of C. When C is 0.18, which was the amplitude of the baseband signal in the experiment, the term does not have a significant effect and is approximately equal to one. The terms of $\cos\phi_{\mathrm{dMM}}$ and $\cos\phi_{\mathrm{dMIC}}$ are the cause of the significant changes in amplitude.

The terms of $(\pi\lambda^2 DLf^2_{\mathrm{MMorMIC}}/c)+\arctan\alpha$ in (2.13) have been studied in relation to fading problems [6]. In our experiment, we used DSF to reduce the fading problems due to fiber dispersion. In the experiment, the microwave and millimeter-wave signals did not have significant fading problems because the dispersion was too small to affect the transmission quality. The length of the first dip was 115 386 and 801 km for the microwave and millimeter waves, respectively, when the dispersion and the chirp parameter were -0.03 ps/nm/km and 0.8.

Next, let us consider the effect of the term $-\arctan[\alpha\cdot C\cdot b(t)/(2+C\cdot b(t))]$ in (2.13). Fig. 13 shows the variation in the term $-\arctan[\alpha\cdot C\cdot b(t)/(2+C\cdot b(t))]$ as a function of C for the dispersion when the chirp parameters are -0.03 ps/nm/km and 0.8. When a large voltage for the baseband signal C is used, the effects of this term become large. This phenomenon can be explained as follows. The RF signals feel the baseband signals as bias voltage. A change in the bias voltage causes fluctuation in the chirp parameters of the optical modulator [10].

In regard to the gigabit Ethernet, there are not always frames to be sent. If there are no frames to send, the baseband signal amplitude C is fixed to -1 or 1. In the calculation, the frequency of the microwave and millimeter wave was set to 5 and 60 GHz, respectively, and their amplitudes were $\mathrm{V}_b=-1.30$ V and $\mathrm{V}_{BB}=0.24$ V, respectively. Moreover, fiber loss was neglected to reveal the effects of dispersion and the chirp of the

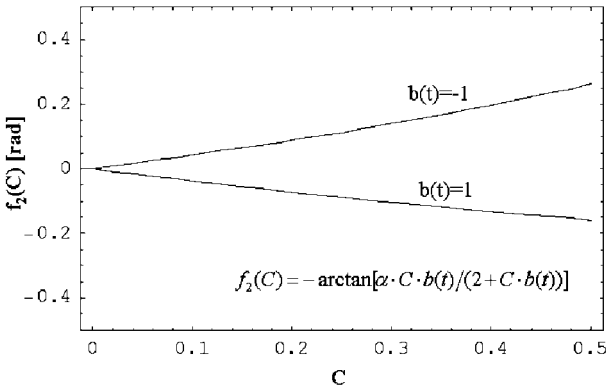

Fig. 13. Variation in term of $-\arctan[\alpha \cdot C \cdot b(t)/(2 + C \cdot b(t))]$ as a function of C.

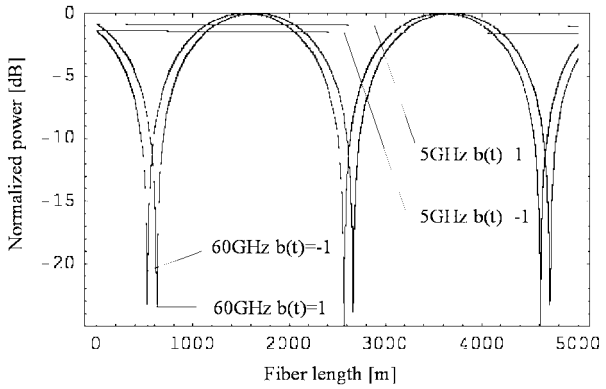

Fig. 14. Normalized power versus fiber length using SMF.

modulator. Fig. 14 shows the mathematical estimation of the detected RF power after an SMF transmission with a dispersion of 17 ps/nm/km. The first dip points of the 60-GHz signal for $b(t) = 1$ and -1 are 625 and 528 m, respectively, where the chirp parameter α was assumed to be 0.8. In these cases, the detected power of the 5-GHz signal is not seriously affected because the first dip point appears at around 76 km. These dip lengths change momentarily according to the amplitude of the baseband signal. The signal power for both millimeter-wave and microwave fluctuates according to the baseband signal. To overcome this problem, the absolute value of the chirp parameter $|\alpha|$ must be decreased by controlling the bias voltage and wavelength of the optical carrier [10]. The amplitude of the baseband signal should then be set as low as possible. We also found that a fiber length of around 1.6 km provided maximum power for the 60-GHz signal without serious degradation of the 5-GHz signal. These analytical results show that if SMF is used as an optical link, the fiber length should be less than 400 m, or 1200–2000 m without any dispersion-compensating technique. With a fiber length of less than 2000 m, the baseband signal will not be degraded [8]. If DSF is used instead of the standard SMF, the limitations on fiber length can be greatly relaxed. Furthermore, optimizing the dispersion parameters maximizes the received RF signal power [10]. Thus, the type of optical fiber selected depends on the size of the network.

VI. Conclusion

We theoretically analyzed and experimentally demonstrated simultaneous multiband modulation and fiber-optic transmission of 2.5-Gb/s baseband, microwave-band, and 60-GHz-band signals on a single wavelength for the first time. The optimum operating conditions for three-band modulation and transmission were obtained for both SMF and DSF. This technique has potential applications in future FTTH access networks combined with wireless access supported by radio-on-fiber wireless feeder.

Acknowledgment

The authors wish to thank N. Otani, T. Itabe, and T. Iida of the Communications Research Laboratory for their encouragement.

References

[1] T. Kamisaka, T. Kuri, and K. Kitayama, "Simultaneous modulation and fiber-optic transmission of 10 Gb/s baseband and 60-GHz-band radio signals on a single wavelength," *IEEE Trans. Microwave Theory Tech.*, vol. 49, pp. 2013–2017, 2001.

[2] D. J. Blumenthal, J. Laskar, R. Gaudino, S. Han, M. D. Shell, and M. D. Vaughn, "Fiber-optic link supporting baseband data and subcarrier-multiplexed control channels and the impact of MMIC photonic/microwave interfaces," *IEEE Trans. Microwave Theory Tech.*, vol. 45, pp. 1443–1451, 1997.

[3] A. Martinez, V. Polo, and J. Marti, "Simultaneous baseband and RF optical modulation scheme for feeding wires and wireline heterogeneous access network," *IEEE Trans. Microwave Theory Tech.*, vol. 49, pp. 2018–2024, 2001.

[4] T. Kuri, K. Kitayama, and Y. Ogawa, "Fiber-optic millimeter-wave uplink system incorporating remotely fed 60-GHz-band optical pilot tone," *IEEE Trans. Microwave Theory Tech.*, vol. 47, pp. 1332–1357, July 1999.

[5] R. B. Welstand, J. T. Zhu, W. X. Chen, A. R. Clawson, P. K. L. Yu, and S. A. Pappert, "Combined Franz-Keldysh and quantum-confined Stark effect waveguide modulator for analog signal transmission," *J. Lightwave Technol.*, vol. 17, pp. 497–502, Mar. 1999.

[6] T. Kuri, K. Kitayama, A. Stöhr, and Y. Ogawa, "Fiber-optic millimeter-wave downlink system using 60-GHz-band external modulation," *J. Lightwave Technol.*, vol. 17, pp. 799–806, 1999.

[7] M. Suzuki, Y. Noda, and Y. Kushiro, "Characterization of a dynamic spectral width of an InGaAsP/InP electroabsorption light modulator," *Trans. IEICE*, vol. E69, no. 4, pp. 395–398, Apr. 1986.

[8] G. P. Agrawal, *Nonlinear Optics*, 2nd ed. New York: Academic, 1995, sec. 2–4.

[9] F. Devaux, Y. Sorel, and J. K. Kerdiles, "Simple measurement of fiber dispersion and of chirp parameter of intensity modulated light emitter," *J. Lightwave Technol.*, vol. 11, pp. 1937–1940, Dec. 1993.

[10] A. Stöhr, K. Kitayama, and T. Kuri, "Fiber-length extension in an optical 60-GHz transmission system using an EA-modulator with negative chirp," *IEEE Photon. Technol. Lett.*, vol. 11, pp. 739–741, June 1999.

Kensuke Ikeda (S'03) received the B.E. and M.E. degrees from Osaka University, Osaka, Japan, in 2001 and 2003, respectively, where he currently is pursuing the doctoral degree in the Graduate School of Engineering.

His research activity and interests are in the areas of radio-on-fiber for millimeter-wave.

Mr. Ikeda is a member of the Institute of Electronic, Information and Communication Engineers of Japan.

Toshiaki Kuri (S'93–M'96) received the B.E., M.E., and Ph.D. degrees from Osaka University, Osaka, Japan, in 1992, 1994, and 1996, respectively.

In 1996, he joined the Communications Research Laboratory, Ministry of Posts and Telecommunications, Tokyo, Japan, where he is mainly engaged in research on optical communication systems.

Dr. Kuri is a member of the Institute of Electronic, Information and Communication Engineers (IEICE) of Japan. He received the 1998 Young Engineer Award from the IEICE.

Ken-ichi Kitayama (S'75–M'76–SM'89–F'03) received the B.E., M.E., and Dr.Eng. degrees in communication engineering from Osaka University, Osaka, Japan, in 1974, 1976, and 1981, respectively.

In 1976, he joined the NTT Electrical Communication Laboratory. In 1982–1983, he was a Visiting Research Fellow at the University of California, Berkeley. In 1995, he joined the Communications Research Laboratory, Tokyo. Since 1999, he has been a Professor in the Department of Electronic and Information Systems Engineering, Graduate School of Engineering, Osaka University. His research interests are photonic networks and radio-on-fiber communications. He has published about 170 papers in refereed journals, written two book chapters, and translated one book. He has received more than 30 patents.

Prof. Kitayama is a Member of the Optical Society of America (OSA), the Institute of Electronic, Information and Communication Engineers (IEICE) of Japan, the Japan Society of Applied Physics, and the Optical Society of Japan. He currently is an Associate Editor on the Editorial Boards of the IEEE PHOTONICS TECHNOLOGY LETTERS and IEEE TRANSACTIONS ON COMMUNICATIONS. He received the 1980 Young Engineer Award from the IEICE of Japan and the 1985 Paper on Optics Award from the Japan Society of Applied Physics.